Study on the Adsorption Feature of Rutin Aqueous Solution on Macroporous Adsorption Resins

Zhenbin Chen,[†,‡,§] Anjie Zhang,[‡,§] Jie Li,[‡,§] Fang Dong,[‡,§] Duolong Di,*[,†] and Youzhi Wu[‡,§]

Key Laboratory of Chemistry of Northwestern Plant Resources and Key Laboratory for Natural Medicine of Gansu Province, Lanzhou Institute of Chemical Physics, Chinese Academy of Sciences, Lanzhou, 730000 Gansu, China, State Key Laboratory of Gansu Advanced Non-ferrous Metal Materials, Lanzhou University of Technology, Lanzhou, 730050 Gansu, China, and School of Material Science and Engineering, Lanzhou University of Technology, Lanzhou, 730050 Gansu, China

Received: October 22, 2009; Revised Manuscript Received: February 3, 2010

The adsorption feature of different kinds of polystyrene-based macroporous adsorption resins (MARs) was investigated systemically at constant temperature employing Rutin as the adsorbate. Different from traditional adsorption patterns, Langmuir and Freundlich adsorption, and the results showed interesting aspects: (1) With the increase of the volume of the initial solution, the adsorption capacity increased to the maximum, and then decreased gradually. (2) Experimental results clearly verified the opinion that the adsorption process of MARs could be divided into three stages—macropores, mesopores, and micropores—by the capillary effects occurring at the two intersections, and the adsorption feature for every stage could be described well by the fourth type of Brunauer model. (3) The model that the inductive effect transmitted to the first layer could not interpret our experimental results reasonably. Thus, the model that the inductive effect passed on to a higher layer was proposed by investigating regression of the experimental results and the conclusion that the inductive effect transmitted to the third layer was drawn.

1. Introduction

As a functional polymeric material, MARs have been shown to be a potentially powerful separation material and have been extensively used in many fields, such as chromatographic analysis,[1] medical treatment,[2] and wastewater disposal.[3] Except for the general advantage as that of the common adsorbent,[4,5] MARs possess more favorable properties such as structural diversity and low cost, which make them more promising.[4−6] To gain greater adsorption capacity and higher adsorption selectivity for some specific organic compounds, chemical modification of the MARs is often adopted by introducing special functional groups onto the matrix of the polymeric adsorbents,[5,6] which would modify the chemical composition of the adsorbent surface and hence improve its adsorption for organic compounds.[7] Thus, investigations of the adsorption feature of organic compounds on MARs are of great importance.[8,9] However, researchers all over the world always paid their attention to the application of MARs, and theoretical research about the adsorption feature of MARs lags severely at present. Although there are several reports about the adsorption feature of MARs,[4,10−13] this research was conducted in solutions that contained several solutes. Because of the adsorbance restriction and the adsorption competition among the adsorbates, the adsorption feature of MARs was not discovered sufficiently. Moreover, instead of investigation of the adsorption feature of MARs systemically, previous reports[4,10−13] simply attributed the adsorption of MARs to the patterns usually used, such as Langmuir and Freundlich. As a result, the state of theoretical research was not improved, which resulted in lacking pertinence at the molecular design in the synthesis and modification process of MARs, and further hampering the development of MARs' research and applications.

Our interest was focused on the adsorption of MARs to flavonoids, and to further investigate the influence of the structure parameters matching degree of MAR and flavonoids on the adsorption feature and adsorption kinetics. Considering the inadequacy in previous reports and combining our research interests, one solute, Rutin, which is one of the classical flavonoids, possesses the representative structure of flavonoids, and is cost-efficient, was adopted as the adsorbate in this work to investigate the adsorption features and the action of the adsorption driving force of MARs systemically. Experimental results showed that the adsorption of MARs was different from that in Langmuir and Freundlich. After referring to the five adsorption patterns presented by Brunauer, we found that the fourth adsorption pattern, which considered the capillary effect, was consistent with the adsorption results of MARs, which was not discovered in the previous solid/liquid adsorption system. To probe the adsorption characters of this adsorption pattern, the adsorption feature was analyzed accurately both in macropores and mesopores by using patterns such as Langmuir, Freundlich, and Wang, and the results proved the pattern of Wang was more suitable for expressing the adsorption feature of Rutin on MARs. However, the goodness of fit (R^2) was less than 0.99 for major MARs. Moreover, the value of the equilibrium constant in the first layer was less than that of the second layer for all experimental MARs, which was contradicted with the basis of the pattern. Through analysis and investigation, we concluded the hypothesis that the inductive effect transmitted to the first layer was unreasonable. Considering the deficiency of Wang, the pattern that the inductive effect passed to a higher layer

* Corresponding author. Phone: +86-931-496-8248. Fax: +86-931-827-7088. E-mail: didl@lzb.ac.cn.
† Chinese Academy of Sciences.
‡ State Key Laboratory of Gansu Advanced Non-ferrous Metal Materials, Lanzhou University of Technology.
§ School of Material Science and Engineering, Lanzhou University of Technology.

10.1021/jp910115q
Published on Web 03/24/2010

TABLE 1: Chemical and Physical Properties of the MARs

resin code	polarity	surface area ($m^2 \cdot g^{-1}$)	average pore size (nm)	average particle radius ($\times 10^{-4}$ m)	true density ($g \cdot mL^{-1}$)	wet apparent density ($g \cdot mL^{-1}$)	pore volume ($cm^3 \cdot g^{-1}$)
LSA30	non-polarity	860	18	3.2	1.00−1.10	0.60−0.70	0.43−0.76
D101	non-polarity	700	30	3.2	1.01−1.05	0.60−0.70	0.44−0.71
LX-68M	non-polarity	1050	13	3.0	1.01−1.05	0.65−0.75	0.38−0.59
LSA40	middle polarity	400	26	3.0	1.01−1.08	0.60−0.70	0.44−0.74
LX28	middle polarity	500	24	2.8	1.01−1.08	0.60−0.70	0.44−0.74
LSA21	middle polarity	630	30	2.8	1.01−1.05	0.60−0.70	0.44−0.71

was proposed. The real terminated layer of the inductive effect was investigated through regression of the experimental results. The regression results both in macropore and mesopore suggested that the inductive effect transmitted to the third layer, which was in accordance with that of the chemical bond.

On the basis of the above work, a novel and more reasonable adsorption pattern for MARs was brought up as follows: (1) The adsorption process of MARs was different from other adsorption materials because of their broad and continuous pore size distribution, and their adsorption feature should be imitated with the fourth pattern of Brunauer, which contained the factor of capillary effect. (2) The adsorption driving force mainly sourced from the surplus valence bonding force of active locus, and the inductive effect of active locus transmitted to the third layer. (3) During the adsorption process, the capillary effect always occurred as the adsorption of MARs altered from macropores to mesopores or from mesopores to micropores. However, it could not be observed clearly unless the adsorbate was infiltrated, while solvent was nonwettable to matrix of MARs.

2. Experimental Section

2.1. Materials. Rutin (chromatographically pure, Nanjing Tcm Institute Of Chinese Materia Medica, Jiangsu, China) and absolute ethanol (AR, Tianjin Baishi Chemical, Tianjin, China) were used in this study, and ultrapure water was obtained from a water purification system (Hitech-Kflow Ultra pure, standard type, Shanghai Hogon Scientific Instrument Co., Ltd. Shanghai, China). Polystyrene type MARs, including LSA21, LSA40, LX28, LSA30, D101, and LX68M, were purchased from Sunresin Technology Co., Ltd., Xi'an P. R. China, and the relative performance parameters gained from the manufacture were listed in Table 1.

2.2. Preparation of Rutin Solution. A 0.16000 g portion (CP225D, 0.01 mg, Sartorius AG, Germany) of Rutin was dissolved into ultrapure water at 80 °C and then brought to volume into a 2000 mL volumetric flask. We pipetted 100.00, 60.00, 45.00, 40.00, 30.00, 20.00, 15.00, and 10.00 mL of the above solution into several 100 mL volumetric flasks and then brought them to volume by ultrapure water, respectively; the solutions with different precise concentrations of Rutin were obtained.

2.3. Determination of the Maximum Absorption Length. The maximal absorption wavelength of Rutin aqueous solution was characterized by a UV spectrophotometer (752N, Shanghai lengguang technology Co. Ltd., Shanghai, China). One of the above prepared Rutin aqueous solutions was added into a cuvette, and the ultrapure water was added to another cuvette as the blank control. The absorptive spectra of Rutin aqueous solution were measured at 2 nm wavelength intervals, and the maximal adsorption wavelength (λ_{max}) was obtained at 360 nm.

2.4. Analytical Procedure of Rutin Solution. The Rutin solution concentration was measured by UV spectrophotometer at 360 nm, and the concentration of raffinate was determined by the obtained standard plotting in the range 0.007−0.04 $mg \cdot mL^{-1}$: $A = 22.1231C$ ($R^2 = 0.9999$), where A and C were the absorbency and the concentrations of Rutin ($mg \cdot mL^{-1}$), respectively.

2.5. Activation and Purification of Macroporous Resins. A certain amount of MAR was added into a conical flask with a cover, and then, ethanol in four times volume of the resins was added; thereafter, the cover was sealed. After steeping for 46 h, ethanol was removed and the activated resins were obtained. To purify the resins effectively, analytical absolute ethanol was used to wash the resins until the white turbidity was not observed as water in three volume times volume was added. Thereafter, the resins were rinsed with ultrapure water until the smell of ethanol was unaware. Filtering the resin and leaving it to dry naturally, the activated and purified macroporous resins were obtained.

2.6. Dynamic Adsorption Experiment. A first study was performed in order to determine the adsorption kinetics of Rutin on MARs, as well as to choose the adsorption time to be used in the study of adsorption isotherm. A 1.00000 g portion of activated LSA21 resin was sealed into a 200-mesh porous bag (2× 6 cm) and placed into a 600 mL conical flask, and then, the conical flask was loaded with 550 mL of 0.072434 $g \cdot L^{-1}$ Rutin solution and fixed to a 30 °C bath temperature oscillator (SHA-B, Jintan Zhengji Instruments CO., Ltd. Jiangsu, China). After adsorbing for certain time intervals, the absorbency of raffinate was detected. This process was sustained until the absorbency decreased to a minimum, and the result showed that the adsorption equilibrium time was 8 h. To ensure all MARs reached the adsorption equilibrium, the adsorption time in the adsorption experiment was prolonged to $t = 10$ h.

2.7. Adsorption Experiment. Six types of polystyrene-based MARs, including middle polarity resins LSA21, LSA40, and LX28 and non-polarity resins LSA30, D101, and LX68M, were adopted to investigate the adsorption feature of MARs. Each above activated resin was averagely shared into 23 portions, and the mass of each portion was about 1.0000 g (dry resin) exactly. Then, each portion was sealed into a 200-mesh porous bag. Thereafter, these porous bags were loaded into different conical flasks, and marinated with different volume solutions in turn, respectively. After sealing with a cover, these conical flasks were placed into a water bath temperature oscillator at 30 °C. We operated the apparatus and recorded the adsorption time until the adsorption equilibrium (10 h) and then the oscillator was stopped. Afterward, the conical flasks were quieted for 20 min at 30 °C. The absorbance of raffinate was measured first. When the absorbance of raffinate was less than 0.2, raffinate was evaporated to the accurate volume that the absorbency of raffinate dropped in the range 0.2−0.8, and the concentration of raffinate at this state was determined according to the working curve. Thereafter, the concentration was translated into the concentration of Rutin in 550 mL, and the equilibrium adsorption capacity was calculated by eq 1.[14]

$$Q_e = (C_0 - C_e)\frac{V_1}{W} \quad (1)$$

where Q_e denoted the adsorption capacity (mg·g^{-1}) at adsorption equilibrium, C_0 and C_e were the concentration of initial solution and the equilibrium concentration of Rutin (mg·mL^{-1}), respectively, V_1 represented the volume of the initial solution (mL), and W stood for the weight of resins (g).

2.8. Determination of Accuracy and Precision. In this experiment, the coefficient of recovery (P) and the relative standard deviation (RSD) were adopted to test the accuracy and the precision of our experimental methods, respectively. P was determined as follows: After the adsorption was finished, the concentration of Rutin (C_1) in raffinate was investigated as that of section 2.7 first; thereafter, 10.00 mL of the standard solution (0.072434 mg·mL^{-1}) was added into a flask loaded with 50.00 mL of the raffinate and the concentration of Rutin (C_2) was determined again. This process was conducted in six randomly selected adsorption experiments, and P was calculated with eq 2.[15]

$$P = \frac{C_2 \times (50 + 10) - C_1 \times 50}{10 \times 0.072434} \times 100\% \quad (2)$$

As for RSD, it was obtained from three parallel experiments, and its value was calculated with eq 3.[15]

$$RSD = \frac{S}{\bar{C}} \quad (3)$$

where C_2 was the concentration of solution in the added standard sample, C_1 was denoted the concentration of raffinate, S stood for the standard deviation, and $\bar{C}$ represented the arithmetic mean value of three parallel experiments.

The values of P and RSD in the experiment were 98.84 and 0.21%, respectively, which indicated that accuracy and precision could satisfy the needs of the experiment.

2.9. Exploration of the Termination about the Inductive Effect. In this work, considering the restriction of pore sizes on the adsorption layer, chromatographically pure Rutin was adopted to explore the termination of the inductive effect on macroporous pores; meanwhile, the adsorption on mesopore was only used to test the suitability of this method. The investigation of the termination about the inductive effect was carried out by using the software program Origin 7.5. The process was conducted as follows: (1) Equations that the inductive effect probably terminated at different layers were deduced, respectively. (2) The results obtained were regressed with the above obtained equations one by one, and the regress results contained the related coefficient (R^2), the equilibrium constant (K_1, K_2, ..., K_n), and the chi square distribution (chi^2/DoF = χ^2/DoF, a Chi-square per degree of freedom, where $\chi^2 = (\Delta_1/\sigma_1)^2 + (\Delta_2/\sigma_2)^2 + (\Delta_3/\sigma_3)^2 + ... + (\Delta_N/\sigma_N)^2$, Δ represented deviation from an experimental point to the fit curve, σ stood for the standard error, and degrees of freedom DoF = number of data points − number of adjustable parameters), were obtained. (3) The above values were conscripted to determine the transmission of inductive effect until the values satisfied with the following conditions, i.e., $R^2 > 0.99$, $K_1 > K_2 > K_3 ... > K_n$, Q_m was in the reliable range, and chi^2/DoF reached the minimum, the regression ended, and the termination layer of the inductive effect was obtained.

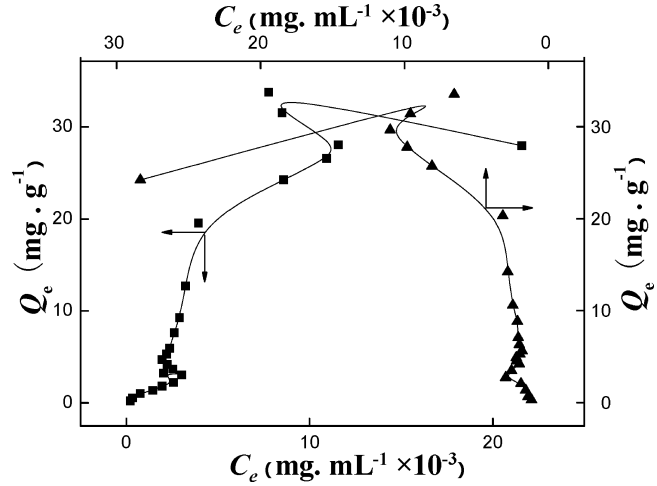

Figure 1. Relationship between Q_e and C_e on macroporous resin (■, altering the concentration while keeping the volume constant (experiment conditions: volume of the initial solution, 550 mL; quality of the resins, 0.9999 g; temperature, 30 °C); ▲, varying the volume while keeping the concentration constant (experiment conditions: initial concentration of Rutin, 0.072434 mg·mL^{-1}; quality of the resins, 0.9999 g; temperature, 30 °C)).

3. Results and Discussion

3.1. Choice of the Adsorption Experiment Methods. To investigate the adsorption feature of MARs in a more detailed manner, the adsorption containing both low and high adsorption capacity should be investigated systematically. Restricted by the solubility of Rutin (0.086 mg·mL^{-1}) and the accuracy range of the spectrophotometer (0.2−0.8), the common method of altering the concentration of initial solution was inconvenient, as it meant a large volume of solution should be used in the experiment to investigate the saturated adsorption. However, a large volume of solution would give rise to solution with a very low concentration in the experiment. The process with both large volume containers and low concentration would complicate and increase errors of the experiment. One well-known way to resolve this problem was to alter the variable of concentration to volume based on the equivalence between the volume and concentration variation,[16] but some inconvenience also existed in this method because MARs could not be covered effectively when the volume of the solution was too small. Thus, the two methods adopted above could not satisfy the requirements. To overcome the deficiency of the two methods above, a novel method should be designed and conscripted. On the basis of this thought, a novel experiment was designed and carried out as follows: If the volume of the loaded stock solution was less than 50 mL, it should be brought to volume into 50 mL with ultrapure water; otherwise, the loaded stock solution was used in the experiment directly. However, a question about the reasonability of this design was presented. To verify the reliability of this design, the relationship between Q_e and C_e in equilibrium of MARs LSA21 was investigated in classical method (i.e., kept the volume of initial solution at 550 mL and altered the concentration of initial solution) and the method designed above (as calculating C_e, the volume was converted into 550 mL), and the results were shown in Figure 1. It could be found that the trends of two curves between Q_e and C_e were almost in accordance with each other, which suggested our design was workable.

3.2. The Adsorption Feature of MARs. Six MARs based on polystyrene, including LSA40, LAS21, LX28, D101, LX68M, and LSA30, were adopted to investigate the adsorption feature.

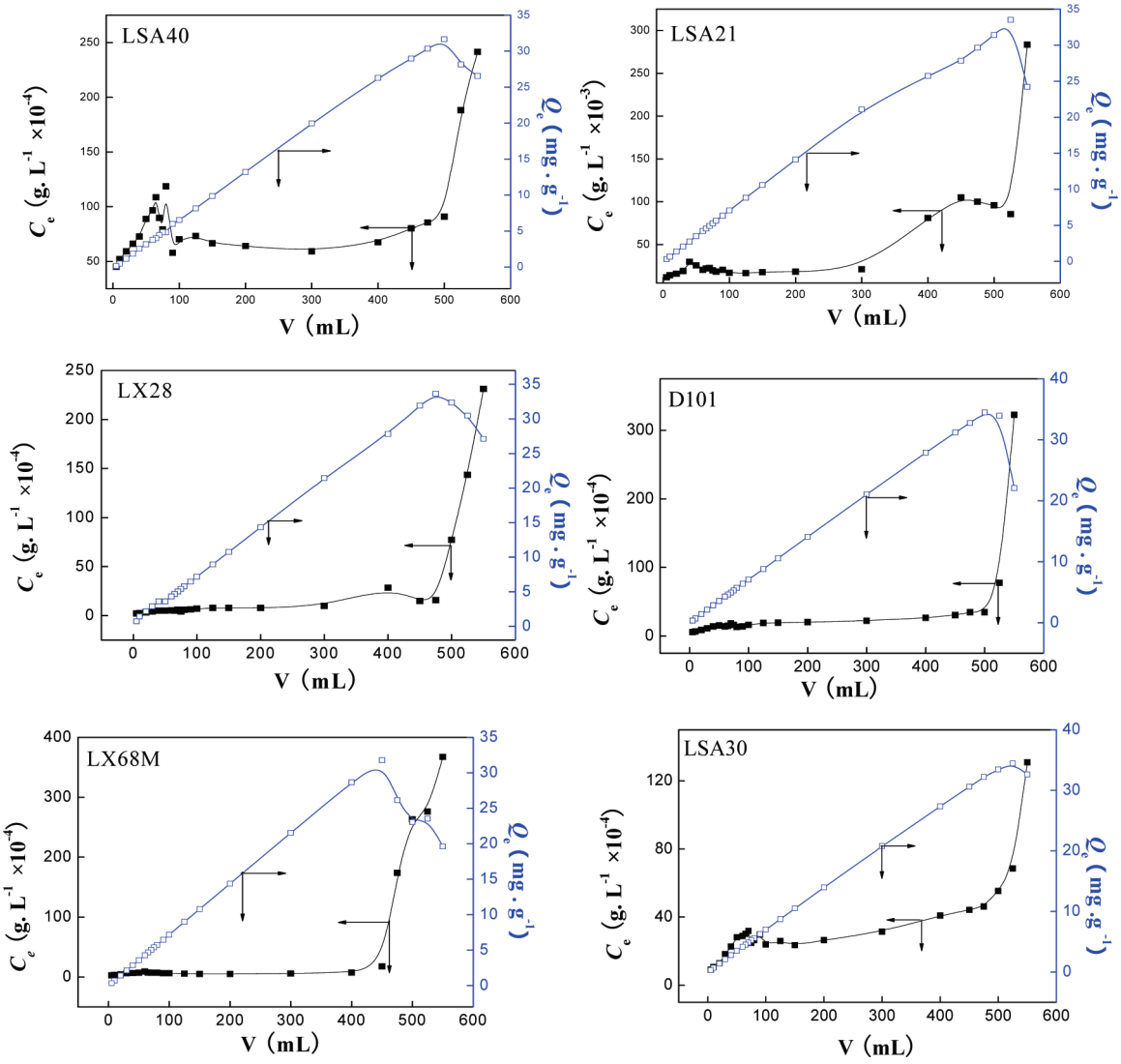

Figure 2. Relationships among the volume of stock solution (V), equilibrium concentration (C_e), and adsorption capacity (Q_e).

The relationships among volume of stock solution (V), equilibrium concentration (C_e), and equilibrium adsorption capacity (Q_e) were shown in Figure 2. It could be found that, with the increase of V, the variation of Q_e and C_e was different. Q_e increased monotonously until it reached a maximum, and then, it would decrease; meanwhile, C_e waved. After Q_e reached a maximum, C_e would increase drastically with the further increase of V. Toward different MARs, the maximum of Q_e and fluctuating point of C_e were different. According to the Langmuir and Freundlich pattern,[17,18] Q_e and C_e increased monotonously with the increase of C_0, deduced from the principle of equivalence between concentration and volume in adsorption aspect;[16] Q_e and C_e should increase monotonously with the increasing of V if the adsorption was obedient to the Langmuir or Freundlich pattern. This suggested the adsorption of MARs did not obey the normal adsorption patterns, i.e., the Langmuir and Freundlich pattern.[13,14]

Figure 2 also suggested the adsorption process of MARs for Rutin was physical adsorption mainly, because it showed a decrease of Q_e and a quick increase of C_e with the increase of V as Q_e reached its maximum.[13]

3.3. The Capillary Effect in the Adsorption of MARs. Figure 3 showed the relationship between Q_e and C_e of different MARs. It also could be found the variation of Q_e and C_e was not positive-going, and it verified that the adsorption of MARs could not be well represented by the Langmuir and Freundlich pattern. To give the difference between the above two patterns and the experimental results, we tried to regress the experimental data using the above two patterns, respectively, and the results were shown in Table 2. A dramatic difference of R^2 among different MARs was found as fitted with the Freundlich pattern, while R^2 fitted with the Langmuir pattern was too low; this also indicated the adsorption of MARs should be represented by another pattern but not Langmuir's or Freundlich's.

The adsorption feature of MARs was determined by their structure, and because of the special preparation, MARs possess many pores in different diameters. Furthermore, many smaller pores existed in the inner face of the larger pores; these pores made MARs present properties that are obviously different from other materials.[17] Besides, due to their particularity in structure, MARs' adsorption also showed a special process: the adsorption first took place on the macropores until all macropores reached equilibrium nearly, and then on mesopores and micropores in turn, until all accessible surfaces of MARs reached their adsorption equilibrium.[18−21] Due to the existence of many capillaries with different pore diameters in MARs and the special adsorption process, the capillary effect should take place inevitably during the adsorption, so the waves of C_e in the adsorption process of MARs could be attributed to the capillary effect during the intersection of two adsorption stages. This

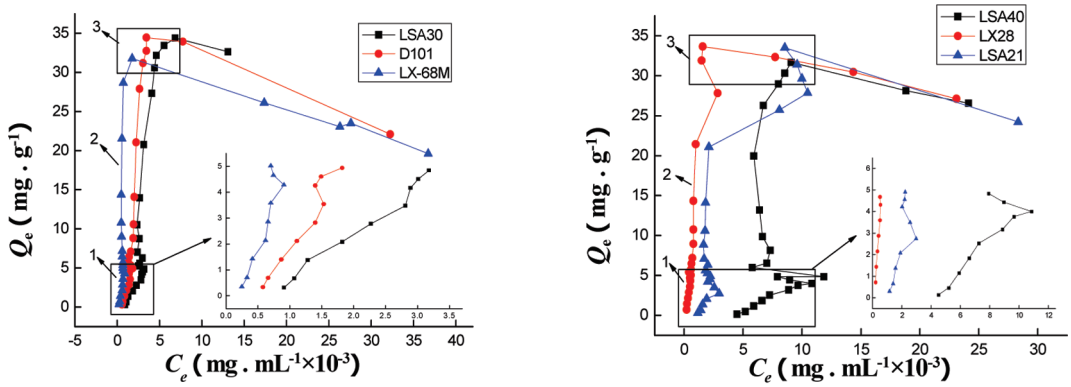

Figure 3. Adsorption isotherm of Rutin on six MARs (experiment conditions: initial concentration of Rutin, 0.072434 mg·mL^{-1}; quality of the resins, 0.9999 g; temperature, 30 °C; 1, 2, and 3 represented the macropore, mesopore, and micropore stages, respectively).

TABLE 2: Regression Results between Q_e and C_e Using the Langmuir and Freundlich Patterns

resin	Langmuir	R^2	Freundlich	R^2
D101	$C_e/Q = 0.289C_e + 3.156 \times 10^{-4}$	0.1911	$\ln Q = 1.167 \ln C_e + 9.201$	0.5796
LSA30	$C_e/Q = -0.097C_e + 9.317 \times 10^{-4}$	0.1614	$\ln Q = 1.084 \ln C_e + 4.204$	0.9994
LX68M	$C_e/Q = 0.041C_e + 1.435 \times 10^{-4}$	0.8610	$\ln Q = 0.487 \ln C_e + 5.180$	0.3689
LSA40	$C_e/Q = -0.418C_e + 7.000 \times 10^{-3}$	0.0739	$\ln Q = 1.850 \ln C_e + 10.707$	0.2560
LSA21	$C_e/Q = 0.005C_e + 5.493 \times 10^{-4}$	0.0016	$\ln Q = 1.073 \ln C_e + 8.136$	0.5158
LX28	$C_e/Q = 0.030C_e + 8.487 \times 10^{-5}$	0.8597	$\ln Q = 0.931 \ln C_e + 3.962$	0.9872

provided a solid experimental basis for the assumption of three adsorption stages.

Many previous reports described the adsorption of MARs by the Langmuir and Freundlich pattern, and the capillary effect was not found in opening reports until now. One of the major reasons might be that the capillary effect was covered up. The infiltrative solution would play an important role in the capillary effect. According to the soakage principle,[22] if the solution was infiltrated to MAR, capillary elevation would take place. Thus, the adsorbate would enter into all accessible pores of MAR more smoothly and be adsorbed on the inner surface of these pores. As a result, if there was not accumulation of adsorbate in solution, C_e would increase monotonously with the increase of concentration or volume, and the capillary effect would be covered up. On the contrary, if solution was not infiltrated to MAR, the adsorbate's entry into MARs would be hampered from larger pores to smaller pores; thus, the concentration of bulk solution would increase. Because the property of solution was determined by both solvent and solute, the increase of solute concentration would vary the infiltration of solution in two ways. (1) If the solute was more infiltrated than the solvent, the capillary resistance would be overcome as the concentration increased to a certain extent; thus, the adsorption in smaller pores would take place and a wave in the relationship between Q_e and C_e or C_e and C_0 (V) would be observed. (2) On the other hand, if the solute was less infiltrated than solvent, the capillary resistance would increase with the increase of concentration, and the adsorption in smaller pores would not take place; thus, few adsorbates would be adsorbed or even none. In this experiment, waves in Figures 2 and 3 illustrated the adsorbate was infiltrated with MARs while solvent was not, which could be interpreted easily if considering the properties of MAR, solvent, and adsorbate.

To prove the wave between Q_e and C_e or C_e and C_0 (V) was caused by the change of the infiltration of solution to MARs, the adsorption experiment of MAR for Rutin alcohol solution was conducted, and the result between Q_e and C_e was shown in Figure 4. It could be found that, as the solvent was infiltrative

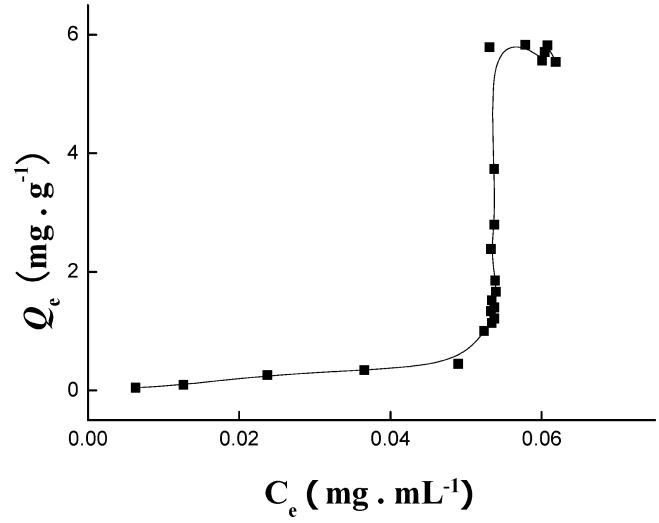

Figure 4. Adsorption isotherm of Rutin on LSA21 in alcohol solution (the experiment conditions were the same as those in Figure 3).

to MARs, the wave of C_e with the increase of C_0 (V) disappeared during the adsorption process.

Figure 3 also showed a quick increase of Q_e after the first wave of C_e, and it could be attributed to the higher ratios of mesopores in MAR.[17,23]

3.4. Investigation of the Adsorption Feature on Macropores of MARs. Since there was a capillary depression effect in the adsorption process of MAR in Rutin aqueous solution, and the adsorption of MARs could be divided into three stages, distinguishing the whole adsorption process into three parts would be facilitating to investigate the adsorption feature of MAR. Whereas the ratios of micropores in MARs were small,[16,22] added to the adsorbate accessible was limited largely, the working points in micropores were too little to analyze the adsorption feature in this stage, so it was not concerned in this work.

Figure 5 and Table 3 displayed the relationship between Q_e and C_e in the macropore stage and the results regressed by the

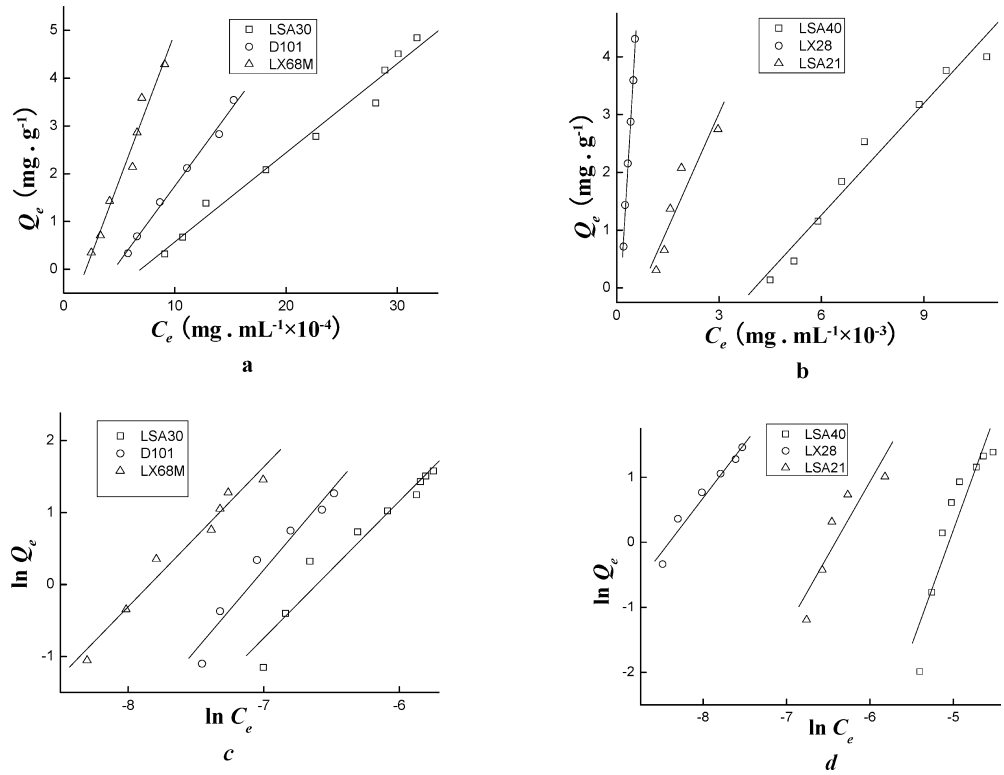

Figure 5. Adsorption isotherm of Rutin on six MARs (a and b were the Langmuir adsorption model, and c and d were the Freundlich adsorption model).

TABLE 3: R^2 Obtained by Langmuir and Freundlich Regression on Macroporous of Adsorption Isotherms

	pattern	
resin	Langmuir (R^2)	Freundlich (R^2)
LSA30	0.5615	0.9448
LSA40	0.4369	0.8506
D101	0.6561	0.9513
LX68M	0.6911	0.9682
LX28	0.6389	0.9602
LSA21	0.419	0.8102

TABLE 4: Results Obtained from the Pattern of Three-Parameter Adsorption Isotherms about MARs

resins	chi^2/DoF	R^2	Q_m (mg·g^{-1})	K_1 (mL·mg^{-1})	K_2 (mL·mg^{-1})
LSA30	0.0652	0.977	228.871	2.914	108.705
D101	0.0377	0.983	198.612	4.595	237.059
LX68M	0.0900	0.972	290.124	7.516	372.811
LSA21	0.1164	0.923	963.641	1.702	53.881
LX28	0.0216	0.989	338.427	13.014	474.455
LSA40	0.1911	0.945	80.280	1.288	48.820

Langmuir and Freundlich pattern about six sorts of MARs. Comparing R^2 of the Langmuir regressions with Freundlich regressions, we could find that all R^2 of Freundlich regressions were higher than those of Langmuir's. This proved the adsorption of the above six MARs was all physical adsorption with multilayers. However, all R^2 regressed with Freundlich were still not ideal, which suggested some features in the adsorption of MARs were still not taken into account by the Freundlich pattern.

To consider the basis of the Freundlich pattern, the adsorption layer and adsorption force were the key to the theory. To overcome the defect of the Langmuir pattern, the Freundlich pattern treated the heterogeneous surface of the practical adsorbent as a homogeneous surface. The surface of the adsorbent was divided into many homogeneous infinitesimal surfaces in terms of adsorption heat, and it assumed the distribution of these homogeneous infinitesimal surfaces was uninterrupted. According to the above ideas, the multilayer concept was brought up and the Freundlich pattern was produced.[24] This pattern enhanced the accordance of regression with experimental results. However, there was also a serious defect in the model, namely, the interaction force among layers was the same. Regarding the defect of the Freundlich pattern above, and basing it on the assumption of the Freundlich pattern, Wang and his co-worker[25] presented a three-parameter adsorption isotherm pattern. This pattern assumed the adsorption process consists of an initial layer adsorption followed by multilayer attachment on previous layers, and there were two adsorption sites: the original solid surface sites for first layer adsorption and the adsorbed adsorbate site for the second and subsequent layer (multilayer) adsorption. For first layer adsorption, the adsorption active energy was supposed as uniform, and one surface site held one adsorbate. Besides, this model granted that the adsorption was reversible. Yu et al.[26] had used the Wang model and obtained a good fitting. In this work, the three-parameter adsorption isotherm pattern was introduced to investigate the adsorption feature of six MARs and the results were shown in Table 4. It could be found a three-parameter adsorption isotherm about MARs was more reasonable than that of Freundlich's. However, some problems existed in this pattern: (1) R^2 for most MARs were still not ideal, $R^2 < 0.99$. (2) According to the hypothesis of the three-parameter adsorption isotherm pattern, the adsorption capacity of different layers decreased with the increase of adsorption layer, which reflected the value of equilibrium constants, i.e., $K_1 > K_2$, but the results calculated from our experiments showed $K_1 < K_2$. (3) All chi^2/DoF values obtained from this pattern were still higher; some were even close to 0.2.

According to the transmission principle of polarity inductive effect on compounds, the polarity inductive effect would not end until it reached the third chemical bond, and the induction force decreased quickly with the increase of transmission space.[27] Similarly, the induction force among molecules also decreased quickly with the increase of transmission space,[28] so the assumption that the polarity inductive effect transmitted to the first layer was unreasonable.

3.5. Determination of the Polarity Inductive Effect Termination. On the basis of the study of Wang and his co-workers and attached to the thought that the induction force could be transmitted to a higher layer, an application program, Origin 7.5, was adopted to probe the information about the transmission of inductive effect. To facilitate the application of the Origin program in this work, the universal expression of the adsorption pattern, which was expressed by the relationship between Q_e and C_e when the induction force was terminated at a certain layer, was deduced, and the deriving process was shown as follows.

For multilayer adsorption, the adsorption of each layer could be expressed using the following general expressions:[25]

$$\begin{aligned} S + M &\leftrightarrow M_1S; \quad K_1 \quad \text{first layer adsorption} \\ M_1S + M &\leftrightarrow M_2S; \quad K_2 \quad \text{second layer adsorption} \\ M_2S + M &\leftrightarrow M_3S; \quad K_3 \quad \text{third layer adsorption} \\ &... \\ M_{n-1}S + M &\leftrightarrow M_nS; \quad K_n \quad n\text{th layer adsorption} \end{aligned}$$

where M denoted adsorbate, i.e., Rutin, S was the free adsorbent surface site, M_jS represented the complex surface, and K_1, K_2, K_3, ..., K_n stood for equilibrium adsorption constants for the first layer, second layer, ..., nth layer, respectively (M^{-1}).

Thus, the equilibrium constant of each layer could be expressed as

$$\begin{aligned} K_1 &= \frac{[MS]}{[S][M]} \quad \text{first layer} \\ K_2 &= \frac{[M_2S]}{[MS][S]} \quad \text{second layer} \\ &... \\ K_n &= \frac{[M_nS]}{[M_{n-1}S][M]} \quad n\text{th layer} \end{aligned} \tag{4}$$

For multilayer adsorption, the adsorbate partially adsorbed by the previous layer was also covered by the subsequent layer adsorbate. This covered adsorbate did not participate in the previous layer adsorption/desorption process. For the previous layer adsorption, only the uncovered part of the adsorbate participates in the equilibrium adsorption/desorption reaction. Thus, $[MS] = XQ_m(\theta_1 - \theta_2)$, $[S] = XQ_m(1 - \theta_1)$, by eq 4

$$K_i = \frac{[M_iS]}{[M_{i-1}S][M]} = \frac{XQ_m(\theta_i - \theta_{i+1})}{XQ_m(\theta_{i-1} - \theta_i)C_e} = \frac{\theta_i - \theta_{i+1}}{(\theta_{i-1} - \theta_i)C_e} \tag{5}$$

where X stood for the total solid concentration ($g \cdot L^{-1}$), C_e denoted the equilibrium adsorbate concentration (M), Q_m was the surface site (monolayer) density ($mol \cdot g^{-1}$), θ_{i-1}, θ_i, and θ_{i+1} presented the fraction of surface coverage at the $(i-1)$ layer, the i layer, and the $(i+1)$ layer ($\theta_0 = 1$), respectively.

Equation 5 could change into

$$\theta_i - \theta_{i+1} = K_iC_e(\theta_{i-1} - \theta_i) \tag{6}$$

Thus, the adsorption equation of the polarity inductive effect transmitted to different layers could be expressed, respectively, as follows:

(1) If there were no transmission of induction force, the adsorption energies for multilayer adsorption would be equal to each other, so the equilibrium constants $K_1 = K_2 ... = K_n$. From eq 6, the following equation could be obtained:

$$\begin{aligned} \theta_1 - \theta_2 &= K_1C_e(1 - \theta_1) \\ \theta_2 - \theta_3 &= K_1C_e(\theta_1 - \theta_2) \\ &... \\ \theta_{n-1} - \theta_n &= K_1C_e(\theta_{n-2} - \theta_{n-1}) \end{aligned} \tag{7}$$

By summing up both sides of eq 7, it yielded

$$\theta_1 = K_1C_e + (\theta_n - K_1C_e\theta_{n-1}) \tag{8}$$

Since θ_n and θ_{n-1} represented the surface coverage at the two outmost layers, and they were small, the term $(\theta_n - K_1C_e\theta_{n-1})$ could be neglected.[25] As a result,

$$\theta_1 = K_1C_e \tag{9}$$

Substituting eq 9 into eq 7

$$\theta_2 = K_1C_e\theta_1 = (K_1C_e)^2 \tag{10}$$

With the same procedure as that of eq 10, the following expression was obtained:

$$\begin{aligned} \theta_3 &= K_1C_e\theta_2 = (K_1C_e)^3 \\ \theta_4 &= K_1C_e\theta_3 = (K_1C_e)^4 \\ &... \\ \theta_n &= K_1C_e\theta_{n-1} = (K_1C_e)^n \end{aligned} \tag{11}$$

Because the total adsorption fraction θ was

$$\theta = \theta_1 + \theta_2 + \theta_3 + ... + \theta_n \tag{12}$$

Substituting θ_1, θ_2, ..., θ_n into eq 12, the relationship between K_1 and C_e was obtained:

$$\begin{aligned} \theta &= K_1C_e + (K_1C_e)^2 + ... + (K_1C_e)^n \\ \theta &= \frac{K_1C_e[1 - (K_1C_e)^n]}{1 - K_1C_e} \end{aligned} \tag{13}$$

Because θ_1 denoted the fraction of surface coverage at the first layer, and the covered surface was always smaller than its inherent surface,[25] $\theta_1 = K_1C_e < 1$ could be gained easily. This meant, as the adsorbent layers were unlimited, $(K_1C_e)^n \approx 0$, and eq 13 could be simplified to

$$\theta = \frac{K_1 C_e}{1 - K_1 C_e} \tag{14}$$

Replacing the surface coverage with the adsorption density, eq 14 could be changed into

$$Q_e = \frac{Q_m K_1 C_e}{1 - K_1 C_e} \tag{15}$$

Equation 15 presented the expression of no transmission of the inductive effect, and it was a two-parameter adsorption isotherm pattern.

(2) Similarly, if the induction force of adsorbent was only transmitted to the first layer, the equilibrium constants of each layer would be equal from K_2, i.e., $K_2 = K_3 ... = K_n$; thus, the adsorption equation was the three-parameter equation, and the equation could be expressed as follows:[25]

$$Q_e = \frac{Q_m K_1 C_e}{(1 - K_2 C_e)[1 + (K_1 - K_2) C_e]} \tag{16}$$

(3) Correspondingly, if the induction force of adsorbent transmitted to the second layer, $K_3 = K_4 ... = K_n$, the adsorption could be expressed as follows:

$$\theta_1 - \theta_2 = K_1 C_e (1 - \theta_1) \tag{17}$$

$$\theta_2 - \theta_3 = K_2 C_e (\theta_1 - \theta_2) \tag{18}$$

$$\begin{aligned} &\theta_3 - \theta_4 = K_3 C_e (\theta_2 - \theta_3) \\ &\theta_4 - \theta_5 = K_3 C_e (\theta_3 - \theta_4) \\ &... \\ &\theta_{n-1} - \theta_n = K_3 C_e (\theta_{n-2} - \theta_{n-1}) \end{aligned} \tag{19}$$

Summing up both sides of eq 19, the following equation was obtained:

$$\theta_3 = K_3 C_e \theta_2 + (\theta_n - K_3 C_e \theta_{n-1}) \tag{20}$$

With the same reason, the term of $(\theta_n - K_3 C_e \theta_{n-1})$ could be ignored. As a result,

$$\theta_3 = K_3 C_e \theta_2 \tag{21}$$

Due to the same procedure, the following equation could be obtained after eq 21:

$$\begin{aligned} &\theta_4 = K_3 C_e \theta_3 = (K_3 C_e)^2 \theta_2 \\ &\theta_5 = K_3 C_e \theta_4 = (K_3 C_e)^3 \theta_2 \\ &... \\ &\theta_n = K_3 C_e \theta_{n-1} = (K_3 C_e)^{n-2} \theta_2 \end{aligned} \tag{22}$$

Now the total adsorption fraction θ could be expressed as eq 12.

The following equation could be obtained by substituting eqs 21 and 22 into eq 12:

$$\theta = \theta_1 + \theta_2 + K_3 C_e \theta_2 + (K_3 C_e)^2 \theta_2 + ... + (K_3 C_e)^{n-2} \theta_2 \tag{23}$$

With the same method, eq 23 could be simplified to

$$\theta = \theta_1 + \theta_2 \frac{1 - (K_3 C_e)^{n-1}}{1 - K_3 C_e} \tag{24}$$

According to the hypothesis of multilayer adsorption, the adsorption capacity of higher layers was smaller than that of lower layers. Thus, $\theta_3 < \theta_2 < \theta_1$ was sure, and $K_3 C_e < 1$ could be acquired effortlessly. With the same condition as that of eq 14, $(K_3 C_e)^n \approx 0$ and eq 24 could be simplified to

$$\theta = \theta_1 + \frac{\theta_2}{1 - K_3 C_e} \tag{25}$$

Substituting eq 21 into eq 18, θ_2 could be calculated as eq 26:

$$\theta_2 = \frac{K_2 C_e \theta_1}{1 + K_2 C_e - K_3 C_e} \tag{26}$$

Introducing the expression of θ_2 into eq 17, θ_1 was obtained as eq 27

$$\theta_1 = \frac{K_1 C_e (1 + K_2 C_e - K_3 C_e)}{(1 + K_1 C_e)(1 + K_2 C_e - K_3 C_e) - K_2 C_e} \tag{27}$$

Substituting the values of θ_1 and θ_2 into eq 25, the relationship between θ and C_e was obtained as eq 28:

$$\begin{aligned} \frac{\theta}{K_1 C_e} = \frac{(1 - K_3 C_e)(1 + K_2 C_e - K_3 C_e)}{(1 - K_3 C_e)[(1 + K_1 C_e)(1 + K_2 C_e - K_3 C_e) - K_2 C_e]} + \\ \frac{K_2 C_e}{(1 - K_3 C_e)[(1 + K_1 C_e)(1 + K_{2e} C_e - K_3 C_e) - K_2 C_e]} \frac{\theta}{K_1 C_e} = \\ \frac{(1 - K_3 C_e)(1 + K_2 C_e - K_3 C_e) + K_2 C_e}{(1 - K_3 C_e)[(1 + K_1 C_e)(1 + K_2 C_e - K_3 C_e) - K_2 C_e]} \end{aligned} \tag{28}$$

Similarly, replacing the surface coverage with the adsorption density, eq 28 could be changed into

$$Q_e = \frac{Q_m K_1 C_e [(1 - K_3 C_e)(1 + K_2 C_e - K_3 C_e) + K_2 C_e]}{(1 - K_3 C_e)[(1 + K_1 C_e)(1 + K_2 C_e - K_3 C_e) - K_2 C_e]} \tag{29}$$

This was a four-parameter equation.

(4) Correspondingly, that the inductive effect transmitted to the ith layer could be deduced with the same method, and it could be expressed as eq 30:

$$\frac{Q_e}{Q_m} = \frac{(1 - K_iC_e)\{(1 - K_iC_e)\sum_{i=3}^{i}[K_1C_e + 2K_1K_2C_e^2 + ... + (i-3)K_1K_2...K_{i-3}C_e^{i-3}] + (i-2)K_1K_2...K_{i-2}C_e^{i-2}(1 + K_{i-1}C_e - K_iC_e)\} + K_1K_2...K_{i-1}C_e^{i-1}}{(1 - K_iC_e)[(1 - K_iC_e)\sum_{i=3}^{i}(1 + K_1C_e + K_1K_2C_e^2 + ... + K_1K_2...K_{i-3}C_e^{i-3}) + K_1K_2...K_{i-2}C_e^{i-2}(1 + K_{i-1}C_e - K_iC_e)]} \quad (i \geq 3) \tag{30}$$

which was an $(i+2)$-parameter equation.

Equation 30 denoted a general formula that the inductive effect transmitted to a certain layer (where $i \geq 3$). Thus, the transmission of the induction force could be investigated from the data of Q_e and C_e obtained from the adsorption equilibrium by Origin 7.5. The relationship between Q_e and C_e was regressed with eq 30. The regression did not end until the corresponding $R^2 > 0.99$, the relative value of K_1, K_2, ..., K_i was in the order of $K_1 > K_2 > ... > K_i$, and the value of Chi^2/DoF reached its minimum. All regression results were listed (see Figure 6 and

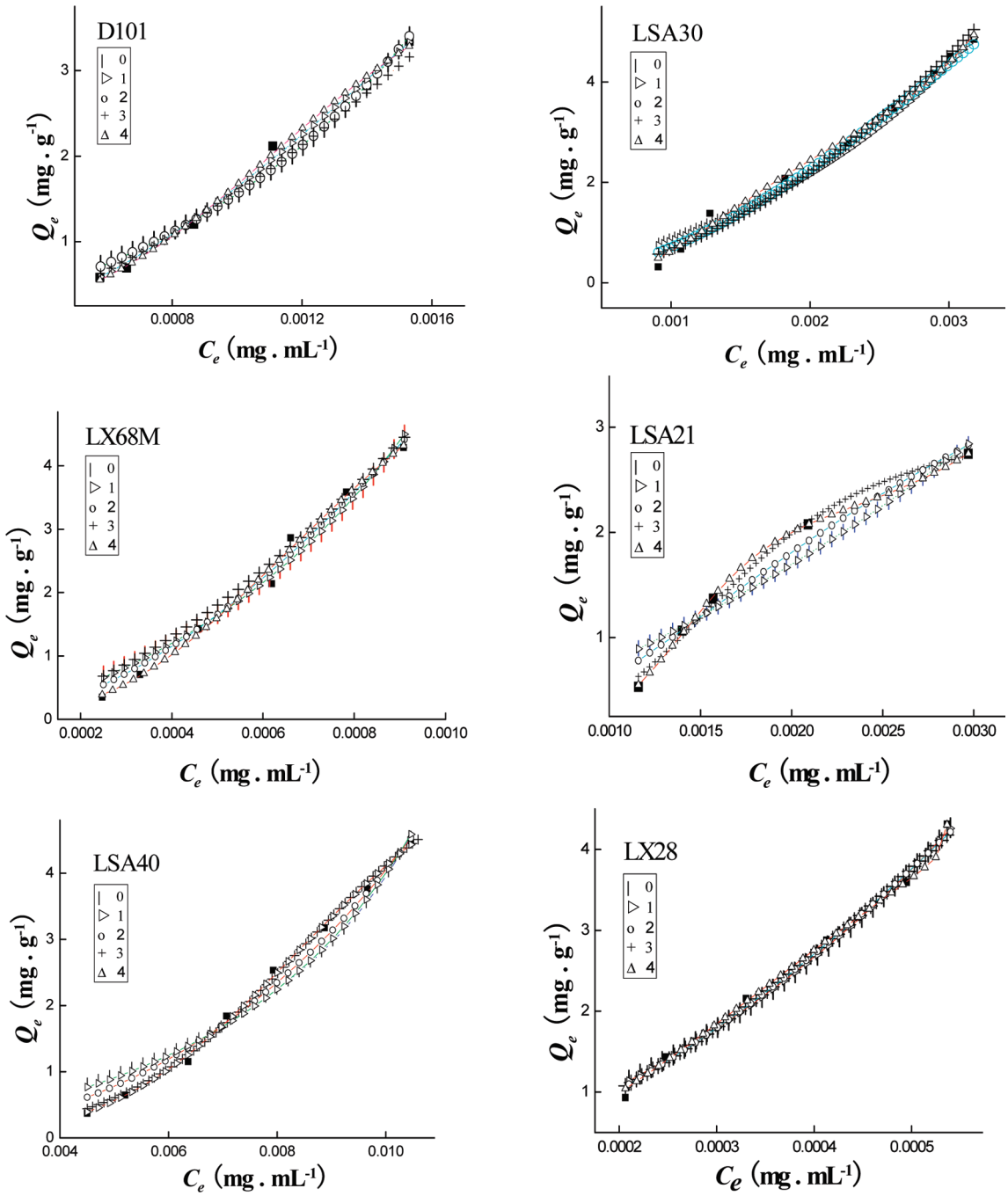

Figure 6. Regression curves of the relationship between equilibrium concentration (C_e) and adsorption capacity (Q_e) in macropores using equations and the induction force transmitted to a certain layer (| - 0, no transmitting of the induction force; right-pointing triangle - 1, the induction force transmitted to the first layer; ○ - 2, the induction force transmitted to the second layer; + - 3, the induction force transmitted to the third layer; △ - 4, the induction force transmitted to the fourth layer).

TABLE 5: Regression Results of the Induction Force Transfer Effect on Macroporous

resins	transmitted layer	chi^2/DoF	Q_m (mg·g^{-1})	K_1 (mL·mg^{-1})	K_2 (mL·mg^{-1})	K_3 (mL·mg^{-1})	K_4 (mL·mg^{-1})	K_5 (mL·mg^{-1})	R^2
LSA30	1	0.0579	4.5244	164.851					0.982
	2	0.0652	228.8710	2.914	108.705				0.977
	3	0.0905	7.0910	33.096	1022.827	53.781			0.980
	4	0.0180	0.4011	700.001	651.898	599.894	30.001		0.990
	5	0.0455	0.5150	0.344	349446.66	2214.49	390.36	562.66	0.994
D101	1	0.0327	2.7555	361.1935					0.980
	2	0.0377	198.6120	4.595	237.059				0.983
	3	0.0175	2.4085	26.618	11632.380	243.502			0.994
	4	0.0112	0.2006	1098.147	1033.094	946.906	18.587		0.991
	5		1.0848	420.66	476.43	1533.997	864.62	462.19	0.996
LX68M	1	0.0807	4.1461	571.4657					0.969
	2	0.0900	290.1240	7.516	372.811				0.972
	3	0.0400	17.0470	58.365	2471.034	36.983			0.991
	4	0.0184	1.4200	1295.807	1119.191	958.612	5.907		0.991
	5	0.1093	2.7215	206.99	1518.22	4451.13	47.647	15.11	0.992
LSA21	1	0.0787	7.3990						0.922
	2	0.1164	963.6410	1.702	53.887				0.923
	3	0.1032	2.0200	1.347	459854.40	59.092			0.966
	4	0.0138	0.1260	2788.095	2494.219	985.843	76.727		0.995
	5		0.1635	0.225	82058.1	11909.23	648.54	821.25	0.999
LX28	1	0.0177	5.8357	67.21742					0.990
	2	0.0216	338.4270	13.014	474.455				0.989
	3	0.0265	38.5420	87.762	1379.763	7.675			0.991
	4	0.0186	1.0730	2993.806	2296.905	1770.384	542.633		0.995
	5	0.0167	4.8728	257.080	8796.54	1.29	901.47	1854.28	0.998
LSA40	1	0.1936	1.9282	67.21742					0.933
	2	0.1911	80.2800	1.288	48.820				0.945
	3	0.1254	3.8190	1.194	15084.552	48.248			0.971
	4	0.0207	0.1360	623.362	387.862	242.152	3.307		0.996
	5	0.0222	1.6994	7.515	43.067	246.615	1146.61	41.98	0.997

Table 5), and it could be found that R^2, K_i order, and Chi^2/DoF were all satisfied with the rules above after regressed to the five-parameter equation. Furthermore, the largest value of Chi^2/DoF was 0.0207, which was much lower than the limited quantity, and it showed an obvious difference from that transmitted to other layers. Besides, R^2 (the lowest value was 0.990) and Q_m (all Q_e were less than the value of Q_m at the inflection point) also showed the five-parameter equation was

TABLE 6: Thermodynamics Results of Induction Force Transmit on Macopores

resins	transmitted layer	$-\Delta G_1^\ominus$ (kJ·mol^{-1})	$-\Delta G_2^\ominus$ (kJ·mol^{-1})	$-\Delta G_3^\ominus$ (kJ·mol^{-1})	$-\Delta G_4^\ominus$ (kJ·mol^{-1})	$-\Delta G_5^\ominus$ (kJ·mol^{-1})
LSA30	1	12.860				
	2	2.695	11.811			
	3	8.816	17.458	10.039		
	4	16.503	16.324	16.114	8.568	
	5	−2.691	28.505	19.404	15.034	15.953
D101	1	14.836				
	2	3.842	13.775			
	3	8.267	23.583	13.843		
	4	17.637	17.484	17.264	7.362	
	5	15.220	15.534	18.480	17.035	15.457
LX68M	1	15.992				
	2	5.082	14.916			
	3	10.245	19.681	9.095		
	4	18.054	17.685	17.295	4.474	
	5	13.434	18.453	21.163	9.734	6.841
LSA21	1	11.427				
	2	1.340	10.044			
	3	0.750	32.846	10.276		
	4	19.985	19.704	17.366	10.934	
	5	−3.755	28.505	23.642	16.312	16.906
LX28	1	16.783				
	2	6.464	15.523			
	3	11.272	18.213	5.134		
	4	20.164	19.496	18.841	15.862	
	5	13.980	22.879	0.642	17.141	18.958
LSA40	1	10.600				
	2	0.638	9.795			
	3	0.447	24.238	9.765		
	4	16.211	15.016	13.829	3.013	
	5	5.081	9.479	13.875	17.747	9.415

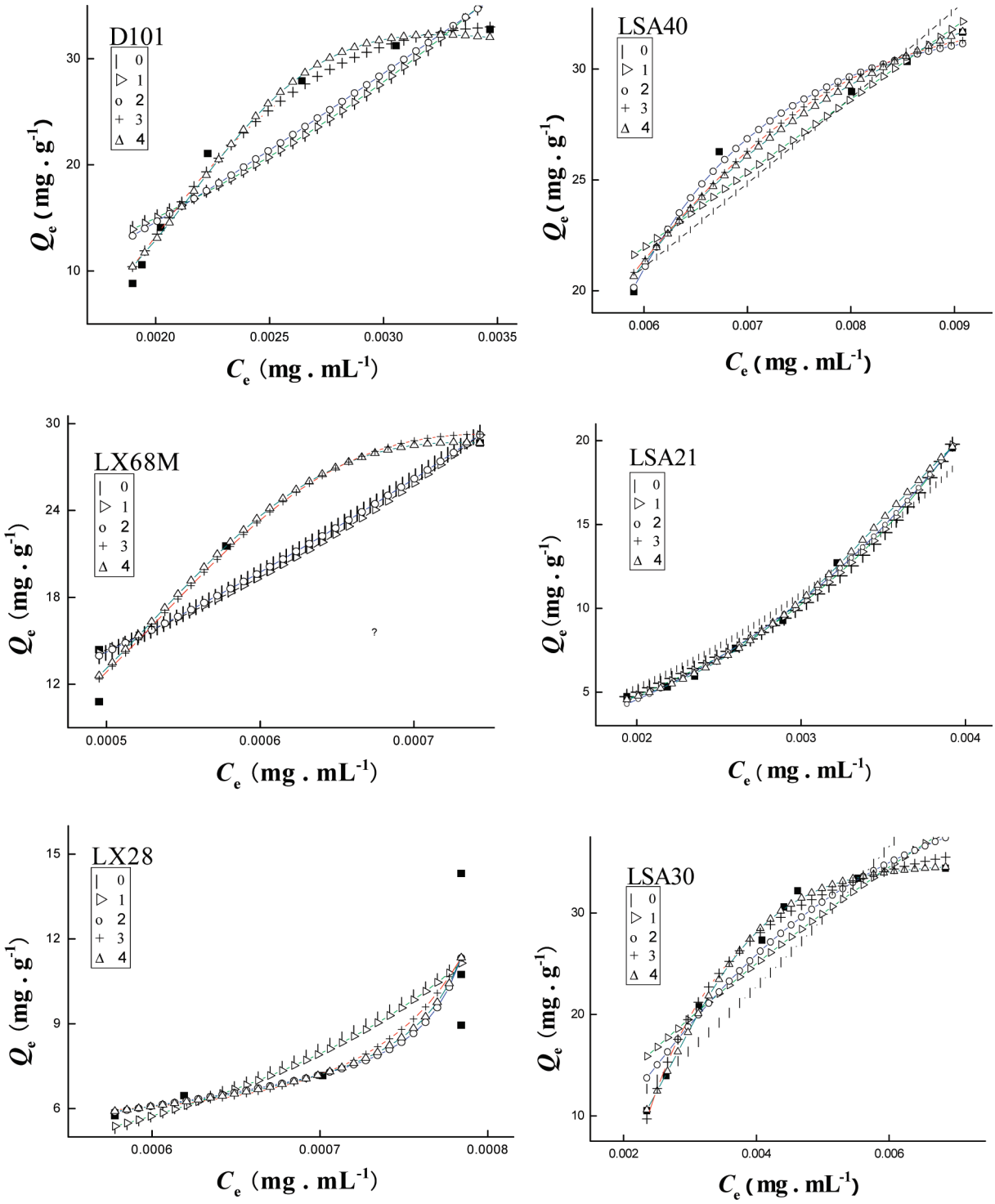

Figure 7. Regression curves of the relationship between equilibrium concentration (C_e) and adsorption capacity (Q_e) in macropores using equations and the induction force transmitted to a certain layer (| - 0, no transmitting of the induction force; right-pointing triangle - 1, the induction force transmitted to the first layer; ○ - 2, the induction force transmitted to the second layer; + - 3, the induction force transmitted to the third layer; △ - 4, the induction force transmitted to the fourth layer).

reasonable. All of the above firmly indicated the induction force of adsorbent would transmit to the third layer, which was in accordance with the transmission of the polarity inductive effect in a chemical bond.[27,28]

3.6. Thermodynamics Evidence of the Polarity Inductive Effect Termination. Table 6 listed the value of $-\Delta G_i$, which was calculated according to the literature.[22,29] It could be found that the difference value between $-\Delta G_3$ and $-\Delta G_4$ was higher than that between $-\Delta G_1$ and $-\Delta G_2$, and that $-\Delta G_2$ and $-\Delta G_3$ were almost equal. This also might indicate the polarity inductive effect would transmit to the third layer. Because the adsorption of MARs belonged to the physical adsorption, according to the literature,[30] the activation energy of the physical adsorption was too small to be considered, and the adsorption/desorption could be carried out easily. Thus, the variation tendency of Gibbs free energy (ΔG) could be used to adjust the environmental change of the adsorption layers directly. In the adsorption process, because of the influence of the polarity inductive effect of interaction sites, the adsorption became easier, K and $-\Delta G$ would increase. With the increase of adsorption

TABLE 7: Regression Results Based on the Induction Force Transfer Effect on Mesopores

resins	transmitted layer	chi^2/DoF	Q_m (mg·g^{-1})	K_1 (mL·mg^{-1})	K_2 (mL·mg^{-1})	K_3 (mL·mg^{-1})	K_4 (mL·mg^{-1})	K_5 (mL·mg^{-1})	R^2
SA30	1	28.056	158.467	30.956					0.718
	2	17.923	98.475	77.938	9.213				0.850
	3	10.924	144.442	46.975	1.327	200.354			0.927
	4	2.452	10.764	437.072	386.071	141.910	31.413		0.939
	5	1.531	8.098	7.530	5996.828	75.035	2015.709	200.727	0.995
D101	1	0.830	41.730	132.996					0.830
	2	0.835	369.985	13.985	91.227				0.835
	3	0.876	21.910	16.285	3535.115	83.482			0.876
	4	3.176	10.096	2282.912	1142.280	625.150	590.497		0.989
	5	8.422	6.051	3.615	133.273	1323.635	19642.455	412.558	0.986
LX68M	1	11.562	25.962	712.819					0.877
	2	22.485	137.652	122.711	523.883				0.881
	3		48.471	168.700	2234.453	415.442			0.892
	4		12.845	2763.421	2356.292	2264.036	69.538		0.893
	5		3.907	186.567	1412.666	1584.821	967.697	1910.769	0.966
LSA21	1	0.2615	9.366	173.114					0.992
	2	0.5245	17.955	79.165	153.477				0.995
	3	2.305	6.362	248.474	236.554	185.693			0.991
	4	2.3812	13.551	324.221	288.297	278.465	72.447		0.996
	5	0.206	2.915	11329.529	44.758	266.198	949.899	319.323	0.999
LX28	1	4.093	5.236	869.597					0.683
	2	5.345	2.996	2882.852	969.033				0.694
	3	7.502	29.916	414.828	2.250	1201.262			0.710
	4	21.117	10.116	623.318	607.954	588.154	75.029		0.714
	5		4.135	6143.518	1387.324	234.356	350.882	1246.393	0.709
LSA40	1	2.620	581.556	5.846					0.909
	2	3.364	58.567	70.526	21.292				0.920
	3	1.311	28.313	15.971	5839.241	440.938			0.922
	4		20.349	3562.063	2675.892	27143.774	2279.388		0.973
	5		4.839	912.240	74.103	150.340	367.779	177.155	0.969

layer, the inductive effect would decrease regularly,[28] and K and $-\Delta G$ decreased correspondingly. As the inductive effect disappeared at a certain layer, the decrease of K and $-\Delta G$ would be more severe and more irregular. In this work, if the adsorption behavior was regressed with a five-parameter equation, the results were just in accordance with the diminishing law of the inductive effect. It also suggested that the induction force of adsorbent transmitted to the third layer was reasonable.

3.7. Investigation of the Adsorption Feature on Mesopores of MARs. In the same method, the adsorption feature of Rutin in a mesopore of MAR was also investigated, and the inductive effect was also analyzed by Origin 7.5 with eq 30. The results were shown in Figure 7 and Table 7. It could be found when the adsorption of MARs was expressed with a five-parameter pattern that the K_i order more satisfied the assumption of the model, and Q_m was more reasonable by comparing with the experimental results, which further proved the opinion that the induction force of adsorbent transmitted to the third layer was reasonable. Compared with the results obtained from the macropore stage, the smaller R^2, higher chi^2/DoF, and disorder of K_3 and K_4 in mesopores could be attributed to the micropore filling principle,[16] which resulted in the random filling of adsorbate in the mesopores after the second layer adsorption, and it led the adsorption capacity to increase dramatically while the increase of equilibrium concentration was small. Besides, the smaller pore sizes of mesoporous would cause the adsorption layers to decrease; thus, the simulation errors caused by the neglected $(K_iC_e)^n$ term would increase. What's more, some pores would be filled fully before the induction force transmitted to the third layer. All reasons above would lead to smaller R^2, higher chi^2/DoF, and disorder of K_3 and K_4.

3.8. Adsorption Pattern of MARs. On the basis of the above work, the adsorption feature of MARs could be described as follows: The adsorption of MARs contained three stages, which were macropores, mesopores, and micropores, and the adsorption feature for every stage could be described well by the fourth type of Brunauer model. The adsorption of organic compounds on MARs in aqueous solution was done through van der Waals force, hydrogen bonding, hydrophobic interaction, and static electrical interaction (including ionic bonds, covalent bonds, and coordinate bonds).[31] Because of the interlaced pore structure in MARs, there was the capillary effect during the adsorption process, which would influence the adsorption feature to a larger extent. If the solution was infiltrated to MARs, the capillary elevation would happen and the capillary effect would be covered up. On the contrary, the capillary depression would take place. Thus, whether the capillary effect could be observed would be determined by the soakage of solute to MARs; if the solute were infiltrated to MARs, the capillary depression could be found clearly at the critical state of the interim from larger pore sizes to smaller pore sizes. However, if the solute was not infiltrated to MARs, the adsorption would only be carried out at the surface of macropores or even no adsorption, and the capillary effect could not be observed. The adsorption of MARs was multilayer adsorption. During the adsorption, the induction force originated from the surface of MARs would transmit to the third layer, and the adsorption could be expressed well by a five-parameter equation pattern.

Acknowledgment. The financial support from program funds of National natural science of China (20974116) and natural science of Gansu (0809RJZA002) are acknowledged greatly.

References and Notes

(1) Tsyurupa, M. P; Malsova, L. A.; Andreeva, A. I.; et al. *React. Polym.* **1995**, *25*, 69–78.
(2) Malik, D. J.; Warwick, G. L.; Venturi, M.; et al. *Biomaterials* **2004**, *24*, 2933–2940.
(3) Yu, Y.; Zhuang, Y. Y.; Wang, Z. H.; et al. *Ind. Eng. Chem. Res.* **2003**, *42*, 6898–6903.
(4) Bulut, Y.; Aydın, H. *Desalination* **2006**, *194*, 259–267.

(5) Huang, J. H.; Zhou, Y; Huang, K. L.; et al. *J. Colloid Interface Sci.* **2007**, *316*, 10–18.
(6) Huang, J. H; Huang, K. L.; Liu, S. Q.; et al. *J. Colloid Interface Sci.* **2008**, *317*, 434–441.
(7) Yang, W. B.; Li, A. M.; Fan, J.; et al. *Chemosphere* **2006**, *64*, 984–990.
(8) Bulut, Y.; Tez, Z. *J. Environ. Sci.* **2007**, *19*, 160–166.
(9) Li, A. M.; Zhang, Q. X.; Chen, J. L.; et al. *React. Funct. Polym.* **2001**, *49*, 225–233.
(10) Chanda, M.; Rempel, G. L. *Ind. Eng. Chem. Res.* **2001**, *40*, 1624–1632.
(11) Silva, E. M.; Pompeu, D. R.; Larondelle, Y.; et al. *Sep. Purif. Technol.* **2007**, *53*, 274–280.
(12) Wang, H. Y.; Zhao, M. M.; Yang, B.; et al. *Food Chem.* **2008**, *107*, 1399–1406.
(13) Zeng, Y.; Li, L.; Yuan, S. D. *Chin. J. Appl. Chem.* **2009**, *26*, 37–41.
(14) Fu, Y. J.; Zu, Y. A.; Li, S. M.; et al. *J. Chromatogr., A* **2008**, *1177*, 77–86.
(15) Li, W. W.; Zhang, H; Li, H.; et al. *Chin. Lab. Med.* **2009**, *24*, 255–259.
(16) Kondo, S. C; Ishikawa, T. S; Abe, I. K.; et. al. *Adsorption Science*, 2nd ed.; Beijing Chemistry Industry Press: 2005 (translated by Li, G. X.).
(17) Ana, M. S.; Oancea, M. R; Dumitru, O.; et al. *Ind. Eng. Chem. Res.* **2006**, *45*, 9096–9106.
(18) Valderrama, C.; Gamisans, X.; de las Heras, F. X.; et al. *React. Funct. Polym.* **2007**, *67*, 1515–1529.
(19) Hopman, R; Meerkerk, M. A; Wiegers, W. G.; et al. *Water Supply* **1994**, *12*, 197–207.
(20) Azanova, V. V.; Hradil, J. *React. Funct. Polym.* **1999**, *41*, 163–175.
(21) Valderrama, C.; Cortina, J. L.; Farran, A. *React. Funct. Polym.* **2008**, *68*, 718–731.
(22) Fu, X. C.; Shen, W. X.; Yao, T. Y. *Physical Chemistry*, 4th ed.; Higher Education Press: Beijing, 1990.
(23) Ye, C.; Gong, Q. M.; Lu, F. P. *Sep. Purif. Technol.* **2007**, *58*, 2–6.
(24) Gu, T. R.; Zhu, B. Y.; Li, W. L. *Surface Chemistry*; Science Press: Beijing, 2001.
(25) Wang, J. M.; Huang, C. P.; Allen, H. E.; et al. *J. Colloid Interface Sci.* **1998**, *208*, 518–528.
(26) Yu, Y.; Zhuang, Y. Y.; Wang, Z. H. *Chemosphere* **2004**, *54*, 425–430.
(27) Yuan, L. B.; Gao, Z. X.; Chen, H. B.; et. al. *Organic Chemistry*; Higher Education Press: Beijing, 1996.
(28) Mai, S. W.; Zhou, G. D.; Li, W. J. *Advanced Structural Inorganic Chemistry*, 2nd ed.; Peking University Press: Beijing, 2006.
(29) Chiou, M. S.; Li, H. Y. *Chemosphere* **2003**, *50*, 1095–1105.
(30) Chen, T. H.; Payne, G. F. *Ind. Eng. Chem. Res.* **2001**, *40*, 3237–3422.
(31) Maity, N.; Payne, G. F. *Langmuir* **1991**, *7*, 1241–1246.

JP910115Q